

**W. H. D. Luna¹,
S. D. Bittencourt³,
M. M. Dias²,
P. M. Aquim²,
R. M. Martins²,
L. Schaeffer³**

J. Electrical Systems 13-4 (2017): 767-778



**Journal of
Electrical
Systems**

Regular paper

**PROCESSING OF SOFT MAGNETIC
MATERIALS BY POWDER METALLURGY
AND ANALYSIS OF THEIR PERFORMANCE
IN ELECTRICAL MACHINES**

This article presents the use of finite elements to analyze the yield of electric machines based on the use of different soft magnetic materials for the rotor and the stator, in order to verify the performance in electric machine using powder metallurgy. Traditionally, the cores of electric machines are built from rolled steel plates, thus the cores developed in this work are obtained from an alternative process known as powder metallurgy, where powders of soft magnetic materials are compacted and sintered. The properties of interest were analyzed (magnetic, electric and mechanical properties) and they were introduced into the software database. The topology of the rotor used was 400 W three-phase synchronous motor manufactured by WEG Motors. The results show the feasibility to replace the metal sheets of the electric machines by solid blocks obtained by powder metallurgy process with only 0.37% yield losses. In addition, the powder metallurgical process reduces the use of raw materials and energy consumption per kg of raw material processed.

Keywords: Powder metallurgy; electric machines; magnetic materials; simulation; magnetization; torque

Article history: Received 31 August 2016, Accepted 10 November 2017

1. INTRODUCTION

Rotating electrical machines can function as a motor or generator and consist of two basic parts, namely the stator and rotor cores. These cores, with rare exceptions, are made from sheet metal (low carbon steel sheets) less than 1 mm thick that are stacked together. Some better performing machines, such as generators, are made from silicon steel sheets of approximately 3% silicon. The entire manufacturing process for these cores basically consists of lamination, stamping, electrical insulation between adjacent sheets, stacking and setting. As to the low carbon steel sheets, the isolation process consists of thermal treatment, where the sheet packages are placed in ovens for some time. Besides relieving stresses, it occurs an oxidation of the sheet surface and, consequently, the formation of an isolating layer of iron oxide between the adjacent sheets. Some types of silicon-steel sheets are supplied by the manufacturers with an oxide based coating on one of the surfaces [1, 2].

* Corresponding author: Ricardo Martins e-mail: ricardomartins@feevale.br

1 Center for Integrated Manufacturing and Technology CIMATEC SENAI – zip code 41650-010, Salvador, BA, Brazil

2 FEEVALE University – P.O. Box 3004, zip code 93525-075, Novo Hamburgo, RS, Brazil

3 Metal Forming Laboratory LdTM – Federal University of Rio Grande do Sul – P.O. Box 15.021, zip code 15021 – Campus do Vale, CEP 91501-970, Porto Alegre, RS, Brazil

W. H. D. Luna, e-mail: wilberth.luna@fieb.org.br; S. D. Bittencourt, e-mail: sergio.bittencourt@ufrgs.br; M. M. Dias, e-mail: moisesdias@feevale.br; P. M. Aquim, e-mail: patrice@feevale.br; R. M. Martins, e-mail: ricardomartins@feevale.br; L. Schaeffer, e-mail: schaefer@ufrgs.br

The rotor and stator cores are surrounded by windings powered by a sometimes alternating electric current, and are subject to the action of induced currents, also known as eddy or Foucault currents, which are responsible for appreciable power loss in these cores. The construction of these magnetic cores from electrically insulated steel sheets partially reduces eddy currents, representing the classic solution for minimizing eddy current losses. However, reduction of induced currents can also be achieved by increasing the electrical resistivity of the core material [1].

It is important to note that, in addition to eddy currents losses, magnetic losses in electromagnetic devices also include hysteresis loss. Thus, alternative materials are currently being investigated to construct these cores as single solid blocks. Desirable primary characteristics for such materials are low hysteresis losses and high electrical resistivity. Moreover, they should also display high saturation induction and magnetic permeability, as well as sufficient ductility to withstand mechanical efforts and the vibration of electrical machine cores [1].

Concerning the soft magnetic materials, these ones are obtained through Powder Metallurgy (P/M) technique in order to replace the traditional stacked laminated steel employed in the rotor and stator cores of rotating electrical machines. More competitive magnetic properties, as some types of small engines with complex geometry and servomotors that operate at high frequency, have been developed using these materials. When one compares electrical machine cores made from electrically insulated iron powders with those constructed using laminated steel sheets, some advantages can be assigned for the former, particularly regarding its isotropic nature in conjunction with unique geometry possibilities, enabling three-dimensional designs [3,4].

Soft magnetic composite materials have two basic structures: resin-coated and microencapsulated materials, with some variations depending on the process used to obtain these materials. Resin-coated magnetic materials are a mixture of powders of ferromagnetic material, such as pure iron, and phenolic resin powders, typically thermoset ones. During the process, the iron powders and resin are mixed, compressed into dies and placed in ovens to cure or plasticize the resin. Thus, the resins act both as an adhesive and electrical insulation between iron particles, increasing the electrical resistivity of the material and reducing Foucault currents (for use in electrical motor cores). In turn, microencapsulated materials consist of depositing some type of electrical insulation, such as a polymer or oxide, on the surface of iron powder particles in the form of films. The procedures employed to deposit insulation are kept secret by manufacturers. For the purpose of forming, the microencapsulated powders are compacted into matrices and placed into ovens for thermal treatment. A variation of both the aforementioned processes is compression molding, in which the forming and consolidation processes occur simultaneously [5].

Concerning the construction, changes in the form and operation of the electrical machines are at the limit of technological improvement and only drastic changes in the materials used for construction of cores will improve their performance, according to information given by design engineers of electrical machines of manufacturers in southern Brazil (WEG Motors and EBERLE Motors).

Therefore, using the Powder Metallurgy processes (P/M), it is possible to construct magnetic cores for electrical machines in massive blocks, with high magnetic permeability (characteristic of magnetic steels) and greater electrical resistivity. However, considering the stator core of an electrical machine, the construction of this package of sheets results in

machines with a higher yield and less loss through eddy current until the frequency of 400 Hz (electrical currents) whenever compared with massive blocks. After 400 Hz, Foucault's current losses in massive cores obtained by M/P become smaller [6,7]. It should be emphasized that certain three-phasic synchronous machines with permanent magnets, as the servomotors, operate with electrical currents of frequencies above 400 Hz.

Another advantage of the use of PM processes is that there are less stages in the manufacturing process of certain parts of the machine (rotor and stator cores), which reduces production costs in manufacturing processes.

In order to predict the performance results of the machines, simulations were done using finite element software FEMM 4.2 (Finite Element Method Magnetics). This is a method that produces purely numerical results. The solution is typically comprised of thousands of points that describe the machine [8]. Yetgin and Turan [9, 10] have been applied the referred method so as to optimize the efficiency of a slitted-core induction motor concerning the slitted structure of the motor.

It should be pointed out that the materials used to construct the stator and rotor cores should present properties such as high relative magnetic permeability, low magnetic coercivity, high electrical resistivity and high induction of saturation.

Thus, in this study it was employed the finite element software (FEMM 4.2) to analyze the yield of electric machines based on the use of different soft magnetic materials for the rotor and stator, built by means of Powder Metallurgy process.

2. MATERIALS AND METHODS

2.1. Procedure to Obtain the Material

Several manufacturing processes are used to obtain magnetic materials. They include foundry and powder metallurgy, which should be mentioned because they are relatively recent processes in this field [11,12].

There are four basic stages concerning the Powder Metallurgy: manufacturing the powder, mixing, compaction and sintering. Sometimes it is necessary milling to perform as a further stage before compaction. In P/M, the powder is compacted into rigid dies where it acquires the shape of the die cavity. After this, the powders are placed in sintering ovens to increase the density and mechanical resistance. It should be mentioned that powders with different chemical natures can be mixed and compacted and a new material is relatively easy to obtain [11,12]. Thus, in this paper, powders with different compositions were obtained by P/M and the properties of the samples obtained are in Table 1. The specification sample 1 (not shown in Table 1) refers to cores with laminated steel sheets. Where \mathbf{B}_r is retentivity, \mathbf{H}_c coercivity, ρ electrical resistivity, μ_r relative magnetic permeability, \mathbf{B} (μ_r) and \mathbf{H} (μ_r) are respectively magnetic induction and field for to calculate permeability.

Table 1 – Sintered materials used in the simulations.

Sample	Sintered alloy	Br [T]	Hc [A/m]	B (μ_r) [T]	H (μ_r) [A/m]	μ_r	P [m Ω .m]
1	M45	-	-	-	-	-	0.370
2	Pure iron	0.355	250	0.230	310	589	0.140
3	Fe-50%Ni	0.108	86	0.055	66	659	0.254
4	Fe-1%P	0.677	320	0.182	98	1.468	0.309
5	Fe-3%Si	0.443	170	0.388	281	1.098	0.196
6	Fe-81%Ni-2%Mo	0.111	52	0.108	81	1.063	0.259
7	Fe-50%Co	0.200	352	0.411	630	518	0.108

2.2. Characteristics of the Materials Applied and the Machine Used.

The relative magnetic permeability, μ_r , of materials is defined as Equation 1.

$$\mu = \frac{B}{H} \Rightarrow \mu_r = \frac{\mu}{\mu_o} \quad \text{Equation (1)}$$

where μ is the real permeability of the material and $\mu_0 = 4\pi \times 10^{-7}$ H/m is the permeability of air. These data are used in simulations.

Ferromagnetic materials have high relative magnetic permeability, which is much greater than 1. So the ferromagnetic materials are extremely important in the construction of electromagnetic devices cores as the rotating electrical machines, transformers and reactors, which work with high magnetic flux for a good performance [13]. Particularly, related to the permanent magnets used in rotor part, they present the following characteristics: 23x3 mm dimensions, 40,5 mm of radius of curvature, 1.23 T of magnetic flux density, 1.099 of relative permeability, 625,000 S/m of bulk conductivity and - 890,000 A/m of magnetic coercivity.

Another characteristic of this type of material is that the relative permeability, μ_r , (shown in Table 1), depends on the magnitude of the magnetic field |H| in the material. This phenomenon is known as the non-linear magnetic behavior and it can be seen in Figure 1 (magnetization curves).

The magnetic properties used in the software are obtained from the magnetization curve that relates magnetic field **H** applied to a material to the resulting magnetic induction **B**. Curves **B x H** for the soft magnetic materials (samples from 2 to 7) analyzed are shown in Figure 1. The test was performed in ring-shaped samples, with primary and secondary windings. with a density of turns in the primary winding of 1319 and 266 turns in the secondary one. The magnetic field H [A/m] was calculated from relation $H.l = N.I$, where l [m] is the perimeter of the ring, I [A] is the primary electrical current and N is the primary number of turns. The induction B [T] was measured in a cross-section of the samples of 0.2 cm² with a Fluxmeter model TLHP-FLX. It should be mentioned that the referred figure

shows the behavior of the materials when the field intensity is raised up to its saturation value.

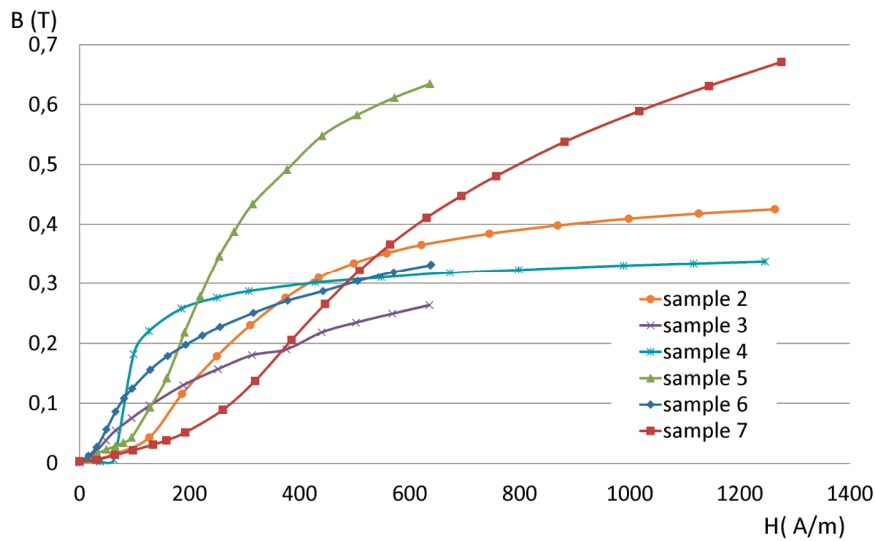


Figure 1 – Magnetization curves of the materials tested.

The machine studied was based on the servomotor SWA-40-1.6-30 model, manufactured by WEG Motors of Brazil and Table 2 shows the main features of the machine.

Table 2 – Real data of the WEG electric machine made in Brazil.

Parameters	Values
I_o	2.0 A
I_{max}	7.2 A
Power	450 W
Turns in Winding	42
Length of cores	40 mm
Mass	2.8 kg
Inertia ($\times 10^{-3}$)	0.084 kg m ²
Length	216.7 mm
SCA-05	4/8
Rated speed	3000 rpm
Stall torque	1.61 N m

Source: <http://ecatalog.weg.net/files/wegnet/1-1769.pdf>

2.3. Pre-Processing

By means of using FEMM 4.2 software, it is possible to verify important data such as instantaneous torque of the electrical machine, the flux concatenated in each coil and the

losses through Foucault current. Once these results are known, the designer can verify the efficiency of the machine and the properties that should be worked on in order to reach the ideal working point.

There are two common sources of magnetic fields (both used in simulation): one of them generated by the current that runs through the copper wires and the other generated by the permanent magnets. One considers a copper wire wrapped over a highly permeable piece of material, called core, in this case applied in the stator. The current that flows through the coil produces a magnetic field which it can be found through the application of the Ampère's law [8]. In the stator of the simulated electrical machine the current applied to circuit 1 and 2 is 2 A and in circuits from 3 to 6 the current is -1 A (the signal represents the direction). Figure 2 shows the details of the configuration of the coils in the machine.

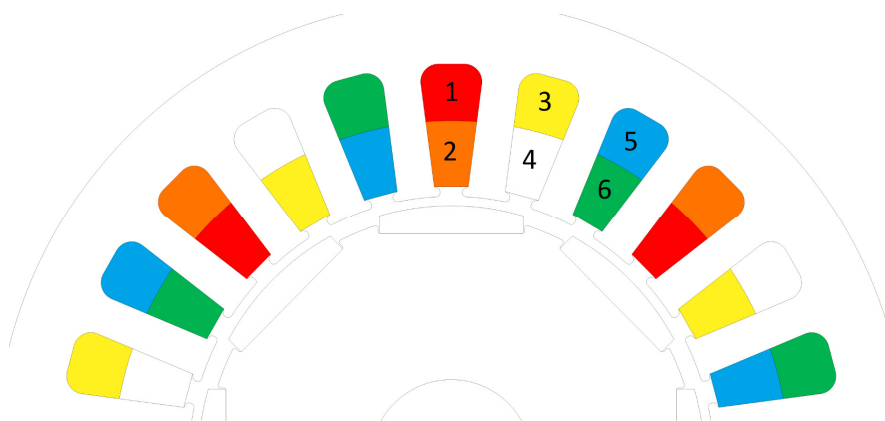


Figure 2 – Configuration of the coils used in the stator.

In FEMM, the domain of the solution is subdivided or “discretized” into small regions called “finite elements”. For instance, in 2D applications, the domain can be discretized into groups of finite areas formed by triangles. The points that define the triangles are the “nodes” or “degrees of freedom”, while the triangle is the “element” itself [13]. The ensemble of elements is called “Mesh”. In the model tested, 100743 nodes and 201173 elements were tested to generate the “mesh”, as it can be seen on Figure 3.

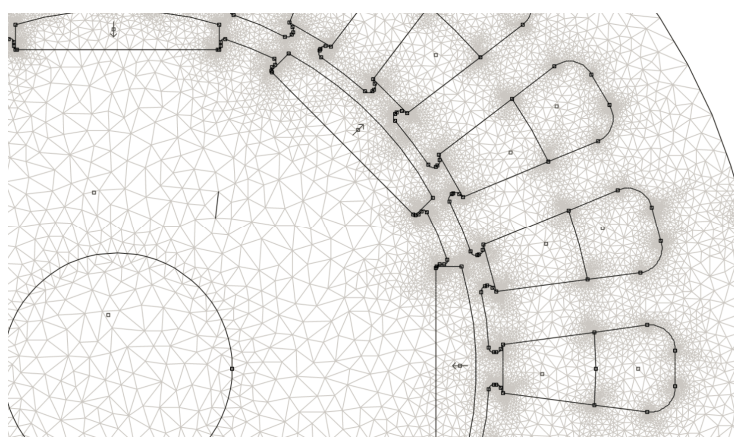


Figure 3 – Mesh generated during pre-processing.

2.4. Data Processing

The torque produced by a magnetic field is based on a macroscopic point of view. The principle used is the concept of energy conservation. This method requires all electrical, magnetic and mechanical losses in the motor (or electrical machine) to be modeled as an external factor to the motor, described in Equation 2. In this meaning, a conservative system is reached, where no energy is lost [8].

$$dW_e = dW + dW_m \quad \text{Equation (2)}$$

where dW_e , dW , and dW_m are differential of energy quantities: electrical, magnetic and mechanical, respectively.

The Maxwell stress tensor describes the force per unit of area produced by the magnetic field on a surface. The differential force produced is described in Equation 3.

$$dF = \frac{1}{2} [H(B \cdot n) + B(H \cdot n) - n(H \cdot B)] \quad \text{Equation (3)}$$

where n denotes the normal direction from the surface to the point of interest [14].

The weighted stress tensor block or simply weighted tensor (Figure 4) is an integral version of volume of the Maxwell stress tensor which automatically chooses an ensemble of pathways to integration, which generates yield results. This approach is similar to the Stress Tensor Approach (WST Weighed Stress Tensor) described in Henrotte [14]. The torque on (0.0) is calculated using the approach of the same weighting function [15].

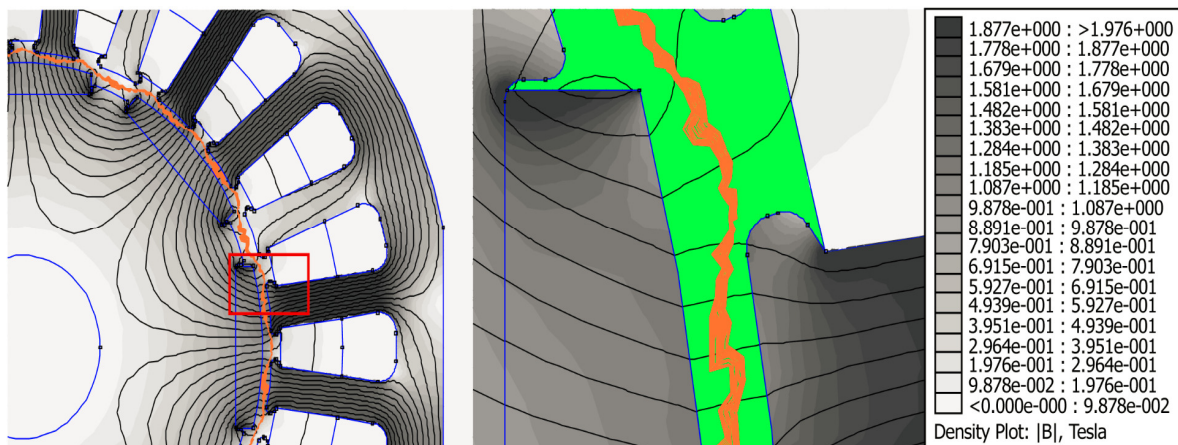


Figure 4 – Torque obtained from the stress tensor (on the left); on the right, the detail of the simulated tensor.

The Weighted Stress Tensor integration is also shown in Figure 4, by patten, as orange flux lines.

3. RESULTS AND DISCUSSION

According to data obtained, it is possible to observe the torque originated by the stress tensor and the torque via weighted stress tensor (Figure 5). The comparative study of the electrical machines will be based on the torque via weighted stress tensor, since its value best represents the yield and it is also the one that comes closer to the nominal value of the electric machine represented.

Sample 1 (M45 – silicon steel) which is part of the database of FEMM 4.2 is used as a reference in the simulations since there is a proptotype model based on this sample. The rotor behavior using this material is similar to the real one. Based on this, it was obtained the first results in Figure 5.

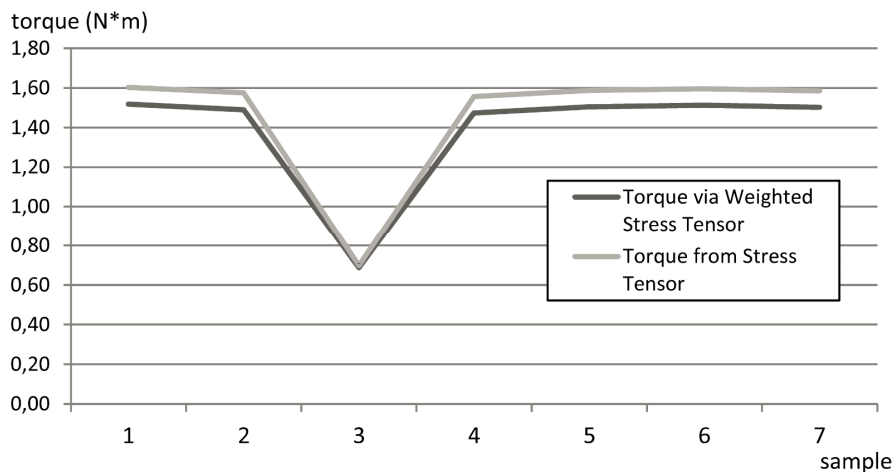


Figure 5 – Torque via weighted stress Tensor vs torque from stress tensor.

Once the torque of sample 3 is very low, if compared to other materials, the yield of the machine under the original conditions (Sample 1) still prevails over other materials. It may be stressed that the samples 5, 6 and 7 are those that have their values closest to the ones related to the reference (Sample 1).

The magnetic potential gradient does not have any physical significance. Its definition comes from a vector calculus law which states that the divergence of a rotational of any vector function is nil. The magnetic potential gradient is known as the magnetic potential vector and its size unit is Wb/m in the International System of Units [16].

The group of samples 1, 2, 4, 5, 6 and 7 presented almost the same two-dimensional field behavior, as it can be observed in Figure 6. These values are directly related to magnetic permeability.

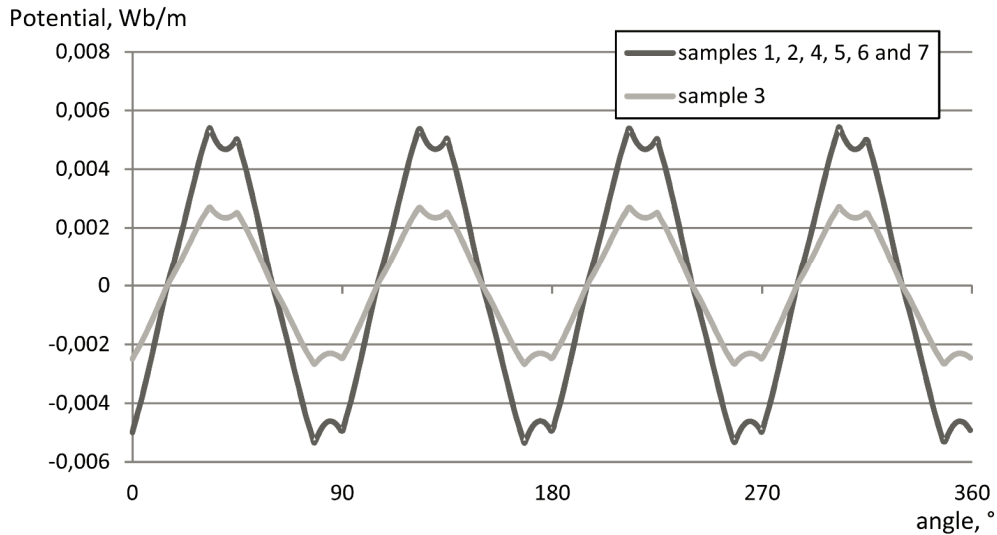


Figure 6 – Measured potential in the airgap,

$B.n$ integral returns the total flux passing normal to the contour. This integral is useful for determining the total flux in a bulk flux path [10]. In Figure 7, a similar behavior is observed as a function of the differences among the materials.

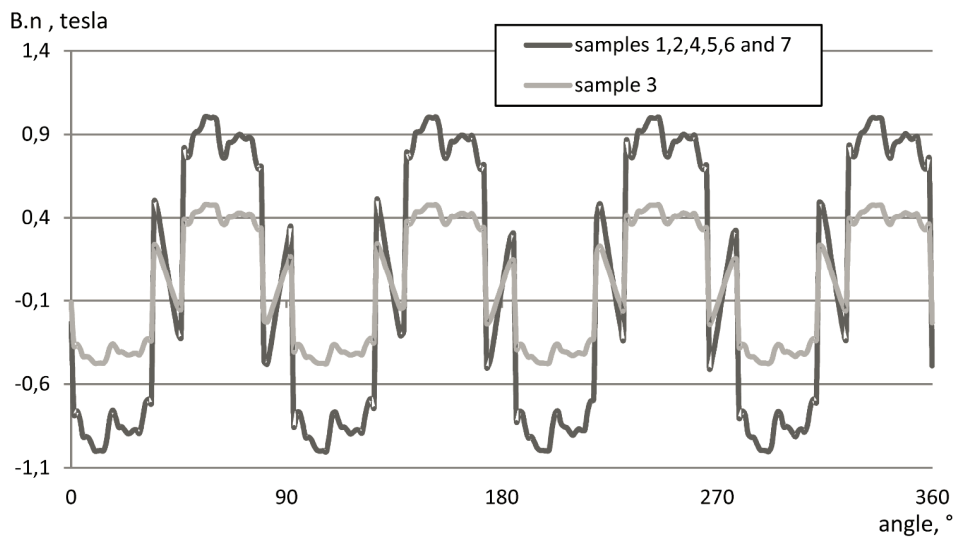


Figure 7 – $B.n$ integral showing the total flux in a bulk flux path.

Figure 8 shows the *magnitude of flux density*. In this case the relation of sample 3 is half that of the others, which would in fact eliminate any application of the material in machines. It should be stressed that in this figure, the materials are subject to an intensity field generated by the own rotor.

This type of results rules out a huge number of possibilities that, from the point of view of production, would be almost impossible to analyze.

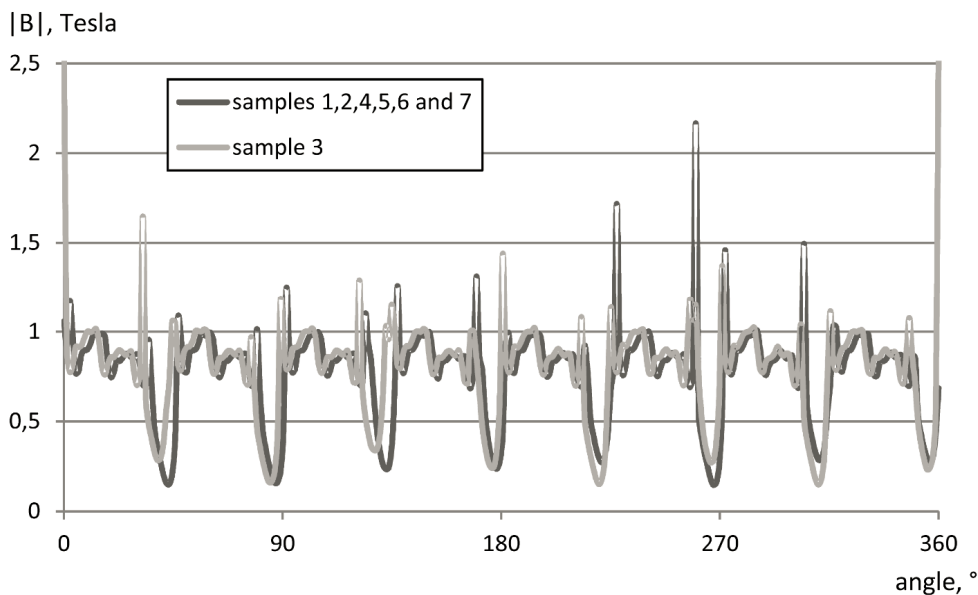


Figure 8 – Magnitude of flux density, in a ratio of 1:2 between the sample 3 and other samples.

All of the previous analysis was performed based on the substitution of the rotor materials. In Figure 9, the material of the stator is also replaced by the material obtained by P/M. In the same figure, the grey columns indicate the torque which can clearly have at most the same yield as the machine where the stator was not changed. In the case of the reference sample (sample 1), and sample 5, there was no difference; on the other hand, in samples 2 and 4 there was a significant decrease in yield.

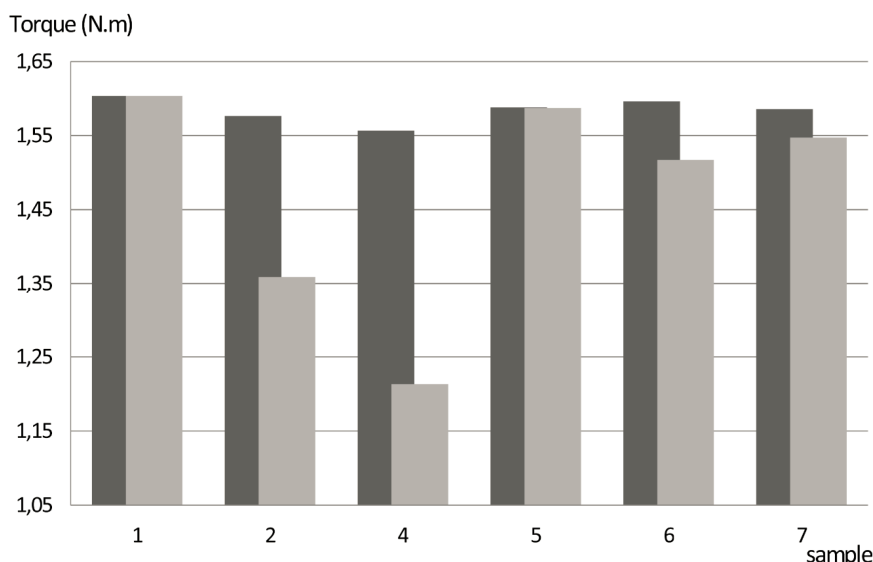


Figure 9 – Analyses of torque from stress tensor in samples 1, 2, 4, 5, 6 and 7. In the black columns, the machines with a rotor obtained by PM and in the grey columns the machines with rotor and stator obtained by PM.

The manufacturing processes of powder metallurgy are much cheaper than the conventional manufacturing processes. The metallic powder is a fraction more expensive than the sheet material, but it can be compensated by diminishing stages in the process of core manufacturing, and by the speed concerning the production of the produced pieces.

The powder metallurgy is a process with high level of utilization of raw material, reaching 95% with an energy consumption of 29 MJ per kg processed; on the other hand, machining processes have losses of up to 50% of raw material consumption and up to 82 MJ of energy per kg processed [17].

Losses due to parasite currents in a massive core are considerably greater than the losses in the cores obtained from electrically isolated sheets. The smaller the thickness of the sheets, the less the parasite currents and the less potency is lost in these cores [1, 2]. In the case of sintered materials, porosity is a typical characteristic. This porosity can be controlled to determine the mechanical properties, but also the magnetic properties, since porosity can increase the electrical resistance of the material, and, consequently, has a relative control of the parasite currents.

4. CONCLUSION

Replacing the stator by materials from powder metallurgy process leads to a slightly decrease in the yield of the machines in almost all cases, although this parameter remained the same for the sample number 5. However, it is possible a reduction of the costs in the manufacturing process owing due to a high level of utilization of raw material and low energy consumption if compared to machining processes.

ACKNOWLEDGMENTS

The authors would like to thank The Brazilian National Council for Scientific and Technological Development (CNPq) for financial support and to the Federal university of Rio Grande do Sul (UFRGS) - Metal Forming Laboratory (LdTM) for the use of their facilities, without which this research would not have been possible.

REFERENCES

- [1] – S.A. Nasar. *Handbook of Electric Machines*. New York: McGraw-Hill, 1987.
- [2] – A.E. Fitzgerald, Jr. C. Kingsley, S.D. Umans. *Electric Machinery*. McGraw-Hill (inc.), 1990: 599.
- [3] – Y.G. Guo, J.G. Zhu, Z.W. Lin, J.J. Zhong. *3D Vector Magnetic Properties of Softmagnetic Composite Material*. Journal of Magnetism and Magnetic Materials 302, 2006: 511–516.
- [4] – E. Enescu, P. Lungu, S. Marinescu, P. Dragoi. *The Effect of Processing Conditions on Magnetic and Electric Properties of Composite Materials Used in Nonconventional Magnetic Circuits*. Journal of Optoelectronics and Advanced Materials 8 2006: 745–748.
- [5] – M.M. Dias, H.J. Mozetic, J.S. Barboza, R.M. Martins, L. Pelegrini, L. Schaeffer. *Influence of Resin Type and Content on Electrical and Magnetic Properties of Soft Magnetic Composites (SMCs)*. Powder Technology 237, 2013: 213-220.
- [6] – P. Jansson. *Soft Magnetic Materials for A.C. Applications*. Hoeganes A.B., Hoeganes Swed." Powder Metallurgy, 1992: 63-66.
- [7] – R.F. Krause, J.H. Bularzik, H.R. Kokal. *Soft Magnetic Material for AC and DC Motor Applications*. Journal of Materials Engineering and Performance v.6, n. 6, 1997: 710-712.
- [8] – D.C. Hanselman. *Brushless Permanent-Magnet Motor Design*. USA: McGraw-Hill, 1994.
- [9] – A.G. Yetgin, M. Turan. *A Novel Slitted Tooth Core Design to Improve the Torque-speed Characteristic of Squirrel Cage Induction Motor*. International Journal of Research in Engineering and Technology. v. 5, n. 5, 2016: 480-487.

- [10] – A.G. Yetgin, M. Turan. *Efficiency Optimization of Slitted-core Induction Motor*. Journal of Electrical Engineering, v. 65, n. 1, 2014: 60-64.
- [11] – S. Bradbury. *Powder Metallurgy Equipament Manual*. New Yersey: MPIF, 1986.
- [12] – R.M. German. *Powder Metallurgy Science*. New Yersey: Metal Powder Industries Federation, 1984.
- [13] – J.P.A. Bastos, N. Sadowski. *Electromagnetic modeling by finite element methods*. USA: Marcel Dekker, Inc., 2003.
- [14] – F. Henrotte, G. Deliege, K. Hameyer. *The eggshell method for the computation of electromagnetic forces on rigid bodies in 2D and 3D*. CEFC, Perugia, Italy, 2002: 16-18.
- [15] – D. Meeker. *Finite Element Method Magnetics*. 2008.
- [16] – A. Nicolaide. *Magnetism and Magnetic Materials*. Transilvania University Press, Braşov, 2001.
- [17] – M.A.T. Pallini, M.A.T. Carvalho. *Cost reduction in the Automotive Industry through Sintering*. Society of Automotive Engineers, 2006: 01-06.